Journal of Energy Chemistry 34 (2019) 171–185

Contents lists available at ScienceDirect

Journal of Energy Chemistry

journal homepage: www.elsevier.com/locate/jechem

http://www.journals.elsevier.com/journal-of-energy-chemistry/

Review

Biomass-derived porous carbon materials for advanced lithium sulfur batteries

Poting Liu, Yunyi Wang, Jiehua Liu*

Future Energy Laboratory, School of Materials Science and Engineering, Hefei University of Technology, Hefei 230009, Anhui, China

ARTICLE INFO

Article history:
Received 13 July 2018
Revised 10 October 2018
Accepted 15 October 2018
Available online 18 October 2018

Keywords:
Biomass-derived carbon materials
Lithium–sulfur battery
Porous carbon
Carbohydrate
Cellulose

ABSTRACT

Biomass, as the most widely used carbon sources, is the main ingredient in the formation of fossil fuels. Biomass-derived novel carbons (BDNCs) have attracted much attention because of its adjustable physical/chemical properties, environmentally friendliness, and considerable economic value. Nature contributes to the biomass with bizarre microstructures with micropores, mesopores or hierarchical pores. Currently, it has been confirmed that biomass has great potential applications in energy storage devices, especially in lithium-sulfur (Li–S) batteries. In this article, the synthesis and function of BDNCs for Li–S batteries are presented, and the electrochemical effects of structural diversity, porosity and surface heteroatom doping of the carbons in Li-S batteries are discussed. In addition, the economic benefits, new trends and challenges are also proposed for further design excellent BDNCs for Li–S batteries.

Poting Liu is currently a postgraduate student in EIT InnoEnergy at KTH Royal Institute of Technology, Sweden. He received his B.E. degree from Hefei University of Technology and had 2-year research experience in Future Energy Lab under the guidance of Prof. Jiehua Liu. His research focuses on advanced materials for sustainable energy systems.

Yunyi Wang is studying for the B.E. degree since 2015 at the Hefei University of Technology, China. She joined in Future Energy Laboratory as an excellent intern student from 2017. Her research focuses on advanced lithium-sulfur battery.

Jiehua Liu received his Ph.D. degree from Nanyang Technological University (NTU, Singapore) in 2011. He carried out the work as a research staff at Institute of Chemistry, Chinese Academy of Science (2007–2008) and NTU (2011–2012). He took up his current position as Professor at Hefei University of Technology at the end of 2012. His current research interests focus on advanced energy materials and high-performance batteries.

1. Introduction

Carbon is one of the most closely related and most important elements for human beings in nature. It is a necessity in people's lives as well as a very important industrial raw material. Because of its diverse electronic orbital properties, carbon materials have a variety of structures and properties [1,2]. New types of carbon materials such as carbon nanofibers [3,4], graphene [5], carbon nanotubes [6], are continuously discovered and artificially produced in these years [7,8]. It can be said that carbon materials almost include the properties of all the materials on the earth, such as the hardest and softest; insulators, semiconductors, and good conductors; thermal insulator and thermal conductor; full absorption–full light transmission [9,10]. With the progress of science and technology, it is found that carbon seems to contain unlimited possibilities of development.

* Corresponding author.
E-mail address: liujh@hfut.edu.cn (J. Liu).

https://doi.org/10.1016/j.jechem.2018.10.005

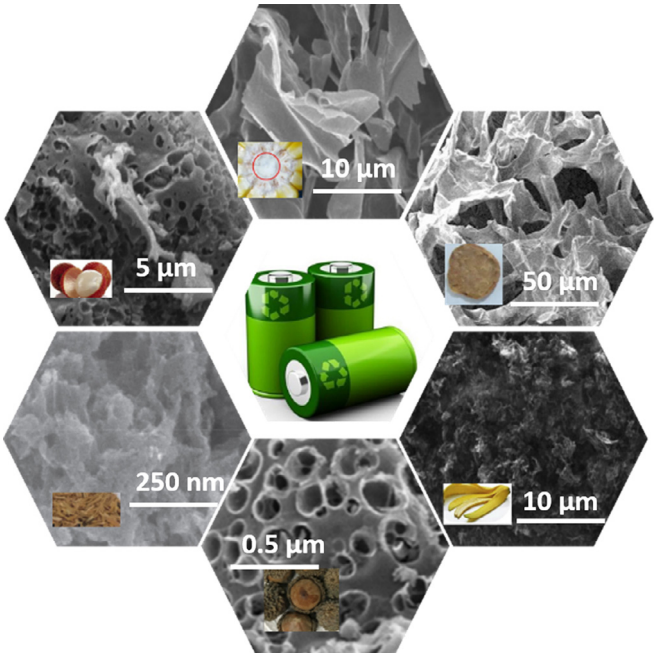

Fig. 1. An overview of the source and structural diversities of biomass-derived carbon materials for Li–S batteries [17–22].

Biomass-derived carbons are made by carbonizing biomass materials such as grass, wood, corn stalks, other crops or crop waste. As the main source of carbon in the world, biomass has optimized the structure of carbon materials in the process of life evolution. It has been found that using it as a raw material can produce porous and highly reactive carbon materials with good physical and chemical stability [11,12]. Biomass-derived novel carbons (BDNCs) usually have high specific surface area and excellent pore size distribution, which can be widely applied in the fields of catalysis, adsorption and energy storage. Among them, applying it to lithium-sulfur (Li–S) battery can effectively improve the electrochemical performance and help overcome shortboard [13–16]. Fig. 1 gives an overview of different sources and structures of BDNCs for Li–S batteries.

The Li–S secondary battery using elemental sulfur as the positive electrode and lithium metal as the negative electrode exhibits a higher theoretical specific capacity (1675 mAh/g) and a theoretical specific energy (2600 Wh/kg), far exceeding the conventional lithium-ion (Li-ion) battery [23–26]. At the same time, elemental sulfur also has the advantages of abundant resources, low cost, and environmental friendliness as a positive electrode material, making the Li–S battery system a hot spot in the new electrochemical energy storage field [27–30]. However, some disadvantages like low sulfur utilization, poor long-term cycling stability, large volumetric expansion and low Coulombic efficiency restrict the applications of Li–S batteries [31,32]. With the development of Li–S batteries, many new research results have been obtained, and many new research methods and ideas have emerged [33–35]. Among them, the research results of the new carbon materials as the carrier of sulfur and the sulfur/carbon composites of the conductive skeleton are particularly remarkable [36–40]. Carbon materials not only have good electrical conductivity, but also have rich hole structure and high specific surface area, which can not only improve the conductivity of composite materials, but also provide the volume space required for the conversion of sulfur into Li_2S_2/Li_2S. The high specific surface area helps to absorb part of the polysulfide and reduce the dissolution of polysulfide in the electrolyte, thereby improving the utilization of active materials and poor cycling performance of the Li–S battery [14,16,41,42]. In this paper, the related research works on Li–S batteries with BDNCs in recent years are reviewed, and the influence of different related factors on the electrochemical performance of Li–S batteries is discussed. Finally, the economic benefits and future development directions of this field are summarized.

2. Preparation and potential of biomass-derived novel carbons

As the main body of nature, biomass can provide us with a very rich carbon source. It is estimated that about 10 to 15 billion tons of biomass wastes are produced annually worldwide, but most of them are not effectively reused, especially agricultural wastes, which are usually disposed of by direct combustion by farmers, not only making the biomass use efficiency less than 20%, but also increasing environmental pollution [43]. In fact, due to the evolution of the natural selection process, carbon nanostructures with abundant species and properties have been formed in biomass. BDNCs can be prepared by simple and appropriate physical and chemical methods and can be widely used as functional materials, providing a new way for the effective utilization of biomass wastes [44,45].

BDNCs are considered as one of the most widely used functional materials because of its rich pore structure, large specific surface area, excellent conductivity, high-temperature resistance acid and alkali resistance [46]. Making full use of BDNCs can not only mitigate catastrophic global climate change, but also increase agricultural productivity and reduce the demand for carbon-intensive fertilizers. The rich pore structure and beneficial microorganisms of BDNCs can make the soil fertile and conducive to the growth of plants. It can also make agriculture more sustainable while increasing crop yields [47].

The most important advantage of BDNCs is the diversity of biomass carbon materials [47–49]. It can use crop straw, forestry processing residue, livestock and poultry manure, organic wastewater from food processing industry, municipal solid waste as raw materials; the preparation methods of biomass carbon materials are simple. Carboniferous materials are heated in an inert atmosphere to remove non-carbon elements such as S, O, H, N and Ca from biomass raw materials; the temperature is usually below 1000 °C. Therefore, biomass carbon materials are widely used in many fields. As a new material, it has a series of excellent properties, such as light weight, high porosity, high-temperature resistance, acid and alkali resistance, good structural stability, easy conductivity, easy heat transfer, easy processing. It can be widely used in high-temperature insulation materials, catalyst carriers, adsorption materials, filter materials and electrode materials of double-layer capacitors and batteries, etc.

2.1. Selection of biomass precursors

In the process of natural selection, the internal structure of biomass is often optimized because of evolution, so carbon materials from biological sources often have high specific surface area and pore volume [13]. The use of modern carbonization technology can further synthesize biological carbon with special shapes and pores, and obtain inherent doped carbon from the actual needs in order to make them exhibit excellent electrochemical performance in the energy storage system [1]. Compared with other advanced carbon materials, BDNCs have attracted wide attention due to its low cost, easy access, and high availability. The carbons obtained from biomass which are applied as cathode materials for S loading in Li–S batteries, can be divided into microporous, mesoporous, hierarchically porous and other special nanostructures such as nanosheets [50,51], 3D architecture [17] and nanofibers [52] carbons according to the structure of BDNCs.

Because of the existence of biodiversity, the carbon which derived from different biomasses usually has unique structures and properties. According to the main components, biomass precursors can be divided into three types [45]: High-sugar and/or high-starch plants, such as cassava [53], litchi [54], corn [55], usually used as precursors to obtain high specific surface area of microporous carbon materials, such as cassava [53], which using as precursor can obtain microporous nano-carbons with high specific surface area of 1198 m^2/g and a small pore volume of 0.67 cm^3/g; Plants rich in cellulose, hemicellulose, and lignin, such as bamboo [19], green algae [56], mangosteen [57,58], usually produce carbon nanoparticles with smaller specific surface areas, but are more likely to have hierarchical pore structures and bigger pore volumes. Taking walnut shell [59] as an example, hierarchical porous carbon materials can be obtained with a high specific surface area of 2318 m^2/g and a large pore volume of 1.13 cm^3/g by high-temperature carbonization. Animals rich in protein and other organic substances, such as fish bones [60], crab shells [61], usually get carbon nanoparticles with large pore volume and high specific surface area. Tuna bone [60] is a good example: porous carbon materials with the large pore volume of 2.53 cm^3/g can be obtained through pyrolysis process.

2.2. Synthesis methods and chemical mechanism of novel carbons from biomass

There are many ways to prepare BDNCs. In order to obtain the best pore size distribution and high specific surface area carbon materials, researchers are constantly innovating in the traditional carbonization technology.

Different carbonization methods will determine the final nanostructures of bio-derived carbon materials due to different chemical mechanisms. Usually, direct carbonization method has certain requirements for the composition and structure of biomass raw materials. The biomass materials with the uniform distribution of mineral elements are more conducive to the formation of porous structure. Otherwise, the carbon materials obtained have poor adsorption performance, so further activation treatment is needed to adjust the pore structure and application of carbon materials. Activated carbonization can not only effectively control the pore size and specific surface area of carbon materials, but also prepare porous carbon materials with different pore types according to different requirements. In the process of hydrothermal carbonization, the porosity and specific surface area of the porous carbon materials are generally low because of the fewer products of hydrolysis and degradation of biomass.

2.2.1. High-temperature direct carbonization (HTDC)

High-temperature direct carbonization (HTDC) refers to the pyrolysis of biomass in an inert gas-protected atmosphere in a vacuum tubular furnace, usually at a temperature of less than 1000 °C [62]. High temperature breaks the C, H and O bonds, and then recombines H_2O, CO_2, and other gas spillovers, thus preparing porous carbon materials with a large number of different pore sizes, which is a traditional method for preparing BDNCs. The process of pyrolysis and carbonization is generally divided into three stages: below 400 °C; 400–700 °C; 700–1000 °C. Relevant studies have shown that when the carbonization temperature is below 400 °C, the main raw material will undergo a decomposition reaction, such as deacidification and dehydration [63]. At this time, the -O- bond does not decompose. However, when the carbonization temperature is between 400 and 700 °C, the -O- bond will break and the oxygen element will be released mainly in the form of CO and CO_2. At the same time, the volatile components of the raw materials will gradually decrease. When the carbonization temperature is 700–1000 °C, the main reaction is dehydrogenation, and finally, a large number of porous carbon materials with different pore sizes are obtained [64].

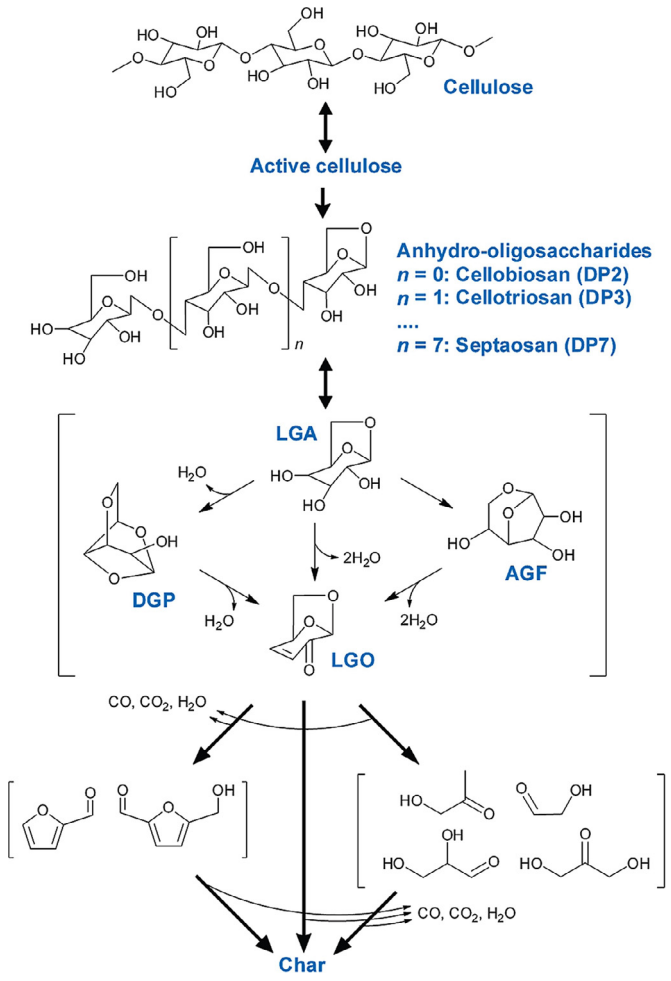

Fig. 2. Proposed mechanism of cellulose pyrolysis (DP indicates 'degree of polymerization') [65].

Liu et al. [65] analyzed the mechanism of cellulose cracking by thermogravimetric analysis and mass spectrometry, as shown in Fig. 2. The results showed that cellulose pyrolysis could be divided into four processes: pyrolysis, dehydration and isomerization, breakdown and condensation of trans-aldehyde alcohol, and polymerization. Gas and coke were mainly due to the breakdown of 1,5-acetal bond C–O–C in dehydrated cellulose. Because the C–O bond was weaker than the C–C bond, the 1,5-acetal bond broke open to form gas and coke at the initial stage of the cracking reaction at the temperature of 300–400 °C. Fracture of C–O and C–C bonds can form a large number of CO and CO_2, leaving four carbon residues. The residual carbon skeleton can form polycyclic aromatic hydrocarbons (PAHs) structure by further cyclization and condensation at higher temperatures. The semi-coke formed at low temperatures has a higher fatty structure and is easier to decompose, while at high temperatures it can form more compact PAHs structure.

2.2.2. Hydrothermal carbonization

As an important driving force for the origin of life, hydrothermal heat is a common phenomenon in nature [66]. At the beginning of the last century, in order to study the formation of coal, the hydrothermal method was used to decompose sugar materials. In 1913, Bergius carbonized cellulose at temperatures of 250–310 °C using a hydrothermal method to obtain a black carbon residue.

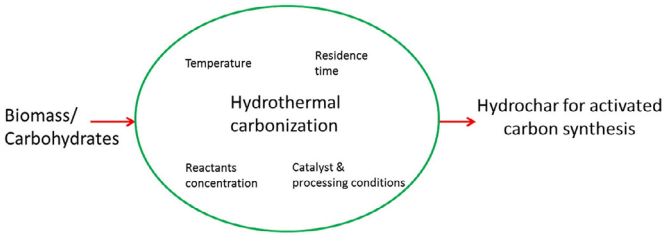

Fig. 3. Factors influencing hydrothermal conversion of biomass [67].

Even now, the hydrothermal method is still a common method for preparing carbon materials [67]. The hydrothermal method is usually carried out in a closed system, using water or an aqueous solution as a medium, heating and pressurizing the reaction system, so that the water or aqueous solution is in a critical or supercritical state, which helps to increase the activity of ions, molecules, etc. in the reactants as shown in Fig. 3. This method accelerates the carbonization process with slow reaction under the normal temperature and pressure, and converts the biomass into carbon materials with various oxygen-containing functional groups and good morphology structure, and has the advantages of environmental protection and simple operation [68,69]. However, hydrothermal and degradation products are less likely to escape in the hydrothermal process of biomass, and the porosity of porous carbon materials prepared by hydrothermal methods is generally low [70].

Recently, Jain et al. reported coconut shell-derived carbon had a larger surface area after hydrothermal pre-treatment, and more oxygenated functional groups than those of reference coconut carbon [71]. However, the formation progress of oxygenated functional groups largely decided on the processing conditions of hydrothermal carbonization. Falco et al. reported an increase in porosity in the corresponding carbons when the precursor was hydrothermally carbonized from 180 to 240 °C due to an increase in carbonyl functionalities up to 240 °C. A further increase in temperature to 280 °C led to enhanced chemical stability and structural order in moisture environment which resulted in a decrease in porosity upon KOH activation [72,73].

2.2.3. Activated carbonization

As described above, it is difficult to prepare carbon materials with high porosity and large specific surface area in one step using direct carbonization method or a hydrothermal method, and the products generally require further activation treatment [74].

The purpose of activation is to change the internal structure of carbon materials, increase their pore volume, and thus improve their properties. The activation method can be divided into physical activation and chemical activation [75]. Physical activation method generally passes through low-temperature carbonization 600 °C, and then through 800–900 °C high-temperature activation. During the process, water vapor, CO_2 and other gases are introduced to protect the material. High-temperature gases react with the material to produce the porous structure on the surface of the material [74].

Generally, the process of carbon activation by gas as a physical activator can be divided into the following five steps [76]: (1) the diffusion of activator molecules from the gas phase to the surface of carbon materials; (2) the diffusion of activator from the surface of particles to the interior of carbon materials through pores; (3) the reaction of activator molecules with carbon to form gas; (4) the gas generated by the reaction expands from the interior of the matrix to the surface of particles; (5) reaction gas diffuses continuously from the surface to the gas phase space. Activated carbon produced by physical activation is simple and clean, and there is no problem of equipment corrosion and environmental pollution.

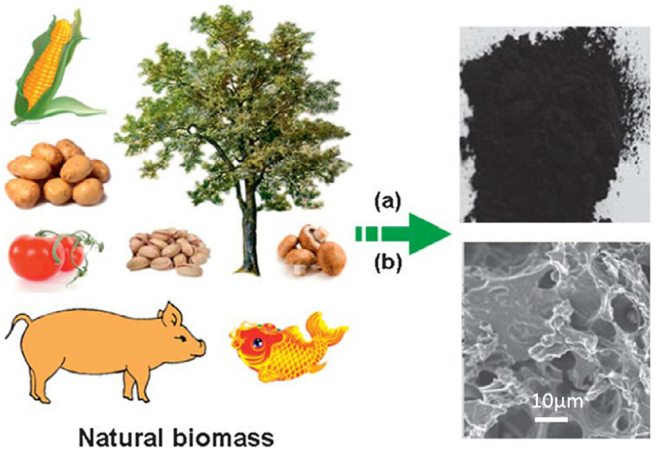

Fig. 4. Transformation of various natural biomass-derived materials into the ACs via (a) pre-treatment followed by (b) KOH activation [79].

Activated carbon products need not be cleaned and can be used directly. Therefore, the activated carbon is usually produced by this activation method in industry, but the reactivity of the gas activator selected by physical activation is relatively weak, and it is difficult to form a developed pore structure in the carbon precursor. Usually, the porous carbon materials prepared by steam activation have a specific surface area of 1000–1500 m^2/g, and the pore volume is less than 1 cm^3/g.

Chemical activation method is to add materials which affect the decomposition process of raw materials, inhibit the tar production of raw materials, thereby preventing the formation of pore plugging. The chemical activation method is completed synchronously at one time and a low reaction temperature. Furthermore, the internal and external uniformity of carbon materials is good and the specific surface area is high. But its pollution and corrosion are strong, and the chemical agents in the materials are easy to remain.

Compared with the physical activation method, the chemical activation method requires a lower reaction temperature [75]. Common chemical activators are KOH (Fig. 4) [54,55,77–79], NaOH [80,81], K_2CO_3 [77,82], $ZnCl_2$ [51,83] and H_3PO_4 [84] etc.

2.2.4. Other carbonization methods

In addition to traditional pyrolysis methods, some new carbonization methods are gradually being developed. Microwave pyrolysis technology has been studied a lot [85,86]. Compared with traditional methods, the heat distribution in the system is more uniform when heated by microwave. Because microwave is the internal heating method, the size of biomass is not limited too much. Some new cracking technologies have also been developed, such as laser [87] and plasma pyrolysis [88]. Laser pyrolysis technology can reduce the amount of sample used, and can quickly raise and lower the temperature, which can effectively avoid the occurrence of secondary reactions. Plasma pyrolysis technology is mainly used to prepare syngas and coke. Compared with traditional methods, plasma pyrolysis technology can greatly improve syngas and reduce the yield of carbon. Although new carbonization technologies have great application prospects, their cost is still high.

Although new carbonization technologies have many advantages, it is not suitable for large-scale production of BDNCs. Considering the factors of carbonization cost, time and quality, high temperature carbonization with corresponding chemical activation is the most suitable and economical method for large-scale industrial production of BDNCs, which requires the design of special high-efficiency, high-yield and low energy consumption biomass

Table 1. The depth of discharge of four phases corresponding to the discharge specific capacity of the sulfur electrode.

Discharge production	Electron transfer number	Depth of discharge (%)	Discharge specific capacity (mAh/g)
$S_8 \rightarrow S_8^{2-}$	0.25	12.5	208.96
$S_8^{2-} \rightarrow S_6^{2-}$	0.33	16.7	275.83
$8S_6^{2-} \rightarrow S_4^{2-}$	0.5	25	417.92
$S_4^{2-} \rightarrow Li_2S_2$	1	50	835.85
$Li_2S_2 \rightarrow Li_2S$	2	100	1671.70

carbonization equipment and more efficient chemical activator to meet the demand of energy saving and environmental protection production. It can be expected that the cost of biomass-derived functional carbon materials produced through industrialization will be much lower than those of other advanced carbon materials, such as graphene [5], carbon nanotubes [6].

3. Biomass-derived carbons in Li–S batteries

Biomass carbon has a very rich pore structure, a large specific surface area, a certain amount of water holding capacity and surface rich functional groups, making it a very wide range of applications in many fields. At present, its application research mainly focuses on environment, energy storage and functional materials. In this section, we focus on the applications of BDNCs in Li–S batteries.

3.1. Fundamentals and challenges of Li–S batteries

A complete Li–S battery is mainly composed of positive electrodes, electrolytes, separators, and negative electrodes. Its cathode material, sulfur, is a coronal structure composed of eight sulfur atoms and has very stable thermodynamic properties. The high charge and discharge properties of sulfur are related to the breakdown and reorganization of sulfur-sulfur bonds in S_8 molecules. During the discharge process, each sulfur atom transfers two electrons, and the number of electron transfer is greater than that of metal ions [32,89–91].

Since the sulfur is in a charged state when the battery is open, the Li–S battery starts to operate with discharge. In the discharge process, lithium ions diffuse from the negative electrode of the battery to the positive electrode and react with the positive electrode material. At the same time, the constantly moving electrons transmit electrical energy through the peripheral circuit. During the charging process, lithium ions and electrons return to the negative electrode and convert the electrical energy into chemical energy [89,90,92–94]. Table 1 shows the depth of discharge of different phases corresponding to the discharge specific capacity of cathode electrode.

There are many reasons why the Li–S battery is hard to put into practical application, mainly due to the positive electrode and the negative pole. In the sulfur positive pole, the main difficulties are as follows. (a) The intermediate polysulfide will dissolve into the electrolyte. During the cycle, the intermediate long-chain polysulfide (Li_2S_4 to Li_2S_8) is easily dissolved in the ether-based electrolyte. Because some active substances always remain dissolved state, they could reach the positive electrode at the end of the discharge [59,90,92]. (b) Low conductivity of sulfur and lithium sulfide. The electrical insulation of sulfur and lithium sulfide and the insulating properties of ion conduction cause the active material not to be fully circulated, and the precipitation of the insulating lithium sulfide during the discharge also leads to the passivation of the cathode surface. (c) Large volumetric expansion of sulfur upon lithiation. Because of the density difference between sulfur and lithium sulfide (2.03 and 1.66 g/cm^3, respectively), sulfur has a larger volume expansion rate when it is become lithium sulfide completely, which may lead to the fracture and damage of the electrode.

In lithium electrode, it is mainly faced with the following difficulties. (a) The shuttle effect of polysulfide. The long chain polysulfide lithium dissolved in the electrolyte can reach the lithium anode, chemically redox, and form low valence compounds, and then these low valence compounds can be returned to the sulfur positive pole again to be reoxidized. This polysulfide shuttle effect occurs inside the battery, causing self-discharge during cycling, resulting in lower Coulombic efficiency. (b) A heterogeneous solid electrolyte intermediate phase (SEI). Lithium metal can react with the electrolyte at the interface of electrolyte and form SEI layer on the surface. The SEI layer is conductive to ionic but electronic insulation. In most cases, SEI is inhomogeneous and does not fully passivate the lithium metal surface, which will lead to a side reaction between the lithium metal and the electrolyte to the consume lithium metals and electrolytes, which leads to the deterioration of the reversibility of the battery, resulting in a lower coulomb efficiency.

In view of the above problems, researchers put forward various solutions, the most common of which is modified packaging of positive materials. The most often used modified packaging materials are carbon materials. However, the carbon material and polysulfide are mainly attracted by weak intermolecular binding force, and the adsorption capacity is weak, resulting in low capture ability of the positive pole to polysulfide [95,96]. In this regard, researchers introduced various functional groups on carbon materials to enhance the attraction of polysulfide and reduce the loss of active substances [36].

BDNCs have excellent mechanical, electrical, thermal conductivity, adjustable pore structure, and rich surface properties which are the required features of cathodes in Li–S batteries. Recent studies have shown that the introduction of BDNCs can greatly improve the performance of Li–S batteries. In the carbon-sulfur composite cathode, nano-carbon materials can form a highly efficient conductive skeleton structure, which can overcome the problem of low conductivity of sulfur and lithium sulfide to a great extent. The unique porous structure of nano-carbon materials can also reduce the loss of active materials and adjust the dissolution, migration and shuttle of polysulfides [13,31].

At the same time, the BDNCs can be prepared into a carbon interlayer with special electrochemical properties, which can further enhance the functionality of the internal separator of the battery. The polysulfide formed will not quickly cross the separator to contact the anode lithium sheet during the charging and discharging process, but can be adsorbed onto the carbon interlayer. The excellent conductivity and self-support of carbon film can make these polysulfides still participate in the charge-discharge process, thus improving the stability and chemical capacity of Li–S battery system. The introduction of BDNCs not only improves the utilization efficiency of sulfur itself, but also adjusts the dissolution and diffusion process of polysulfide in the system, inhibits the formation of lithium dendrite, and plays a multi-function of conductive agent and binder. BDNCs provide a new broad space for the construction of efficient Li–S battery system.

Table 2. Porous carbons derived from high-sugar/high-starch biomass used as key materials and their properties for Li–S batteries.

Biomass source	Obtained structure	Activating agent	Surface area (m^2/g)	Pore volume (cm^3/g)	Initial capacity (mAh/g)	Capacity retention (mAh/g)	Cycle number/ rate (C)	S (wt%)	Ref.
Corncobs	microporous nanosheets	KOH	1198	0.672	1600	634	50/0.1	44	[55]
Chitosan	mesoporous	/	1290	1.29	1163	715	100/0.2	60	[97]
Litchi shell	mesoporous	KOH	1438	/	1667	612	200/0.5	50	[54]
Waste coffee grounds	hierarchical porous carbon	$ZnCl_2$	1017.5	0.48	1150	613	100/0.2	47.6	[83]
Cassava*	macroporous sheet	/	13.8	0.015	1318	811	100/0.5	60	[53]

* Derived carbons used as interlayers.

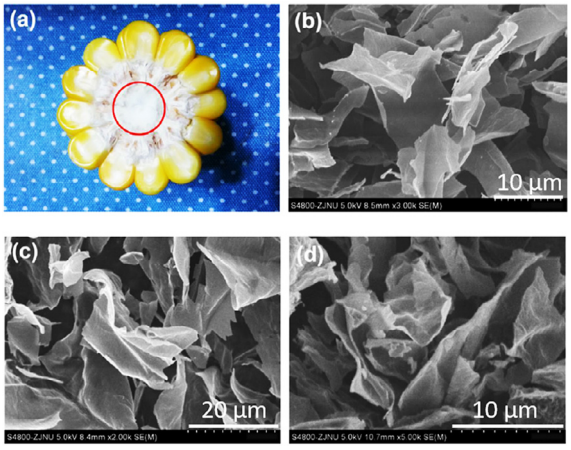

Fig. 5. (a) Digital photos of corn; (b, c, and d) SEM images of products carbonized at 500 and 900 °C from Ref. [55].

3.2. Biomass-derived carbon from high-sugar and/or high-starch plants

Sugars are usually referred to as polyhydroxy aldehydes or ketones. Chemically, they are composed of carbon, hydrogen and oxygen elements, and behave similarly in chemical form to the polymerization of carbon and water, so they are also called carbohydrates. The general formula is $C_n(H_2O)_m$. Most plants first synthesize glucose through photosynthesis and then convert it into starch. The most common high-sugar and high-starch biomass include sugarcane, cassava, corn and litchi etc. Carbons derived from such biomass usually have small pore volume, which can significantly control the shuttle effect in Li–S batteries and improve the cycle performance. It can also be made into special thin films to provide channels for ion transport inside batteries. The applications of high-sugar/high-starch BDNCs in Li–S batteries are shown in Table 2.

Guo et al. [55] used corncob waste material as a carbon source. They activated the corncob with KOH and annealed it at 500 °C and 700 °C respectively to create sheet-like two-dimensional with a microporous structure which leads to the high utilization of sulfur. Excellent electrochemical properties, such as high initial capacity (1600 mAh/g) and a reversible capacity of 554 mAh/g were attained in the sample. The highly porous structure of two-dimensional carbon nanosheets, as shown in Fig. 5, not only enabled stable and continue pathway for rapid electron and ion transportation but also restrained soluble polysulfides and suppressed the “shuttle effect”.

The porosity of carbon materials have a very important effect on the electrochemical performance, which directly determines the utilization efficiency of electrode active substances, but it is usually very difficult to control porosity during carbonization. Zhou et al. [97] put forward a new method of tunable porosity for BDNCs. They employed a mass-producible spray-drying process to prepare mesoporous carbon spheres (MCSs) using chitosan as carbon precursor with ethanol as porosity tuning agent as shown in Fig. 6. The MCSs with different porosities were deduced through the treatment of the volume ratio of ethanol in chitosan solvent. By controlling the volume ratio of ethanol in the solution, and no pore guiding agent or template been introduced, three kinds of MCSs with the controlled specific surface area from 645 to 1292 m^2/g and pore volume from 0.33 to 1.29 m^2/g were obtained. By a melt-diffusion technique, the MCSs with 50 wt% sulfur loading composite cathodes were obtained, and they displayed good electrochemical performance, such as hold initial discharge capacity of 1163 mAh/g, excellent rate capability of 510 mAh/g at 2C and good cycling stability of 715 mAh/g after 100 cycles at 0.2 C.

As previously described, the BDNCs obtained by KOH activation method are usually capable of obtaining an ultrahigh specific surface area and good pore size structure. Sun et al. [54] synthesized novel mesoporous carbon materials with excellent electron conductivity and high surface area successfully from waste litchi shells. They found that there are many porous irregular channels in the lychee shell, which allows KOH to easily enter the inner channel, thus improve its activation efficiency and create more porosity with the high surface area. The as-prepared carbon possessed a large pore volume of 1.88 cm^3/g and ultrahigh surface area of 3164 m^2/g. What’s more, the carbon exhibited similar electron conductivities to conductive carbon black. In order to further explore the electrochemical performance, the carbon was employed as sulfur host matrix and the composite was obtained by the traditional melt-diffusion technique with 60 wt% S loading. Contributed to the abundant network porous structure inside the carbon, the material had a high specific surface area and pore size distribution, which makes the composites high S content and uniform distribution. The available nanostructure effectively suppressed the dissolution of polysulfides. Due to the excellent structural parameters of this porous carbon, very promising electrochemical results were obtained. The composite delivered a high initial specific capacity of 1667 mAh/g and remained 612 mAh/g after 200 cycles at a high current density of 0.5 C, and showed long-term capacity retention of 51% after 800 cycles.

Zhao et al. reported a facile strategy to synthesize oxygen and nitrogen co-doped porous carbon (ONPC) by one-step pyrolysis of waste coffee grounds. The as-prepared carbon possessed an abundant surface area of 1017.5 m^2/g, a high pore volume of 0.48 cm^3/g, and it owned highly rich micro/mesopores as well as abundant oxygen and nitrogen co-doping. The carbon was used as a sulfur host via a solvothermal synthesis method. The hierarchical porous framework and oxygen/nitrogen co-doping can capture the polysulfide through strong chemical binding. The composite showed a high utilization of sulfur and a good electrochemical performance. The existence of the O/N-doped functional groups resulted in the good interfacial adhesion between the active materials and the electrolyte and restrained active sulfur material loss. In addition, the hierarchical porous structure of the composite provided moderate to large pore volume and specific surface area, which suppressed the composite interface damages and the abuse of volume change during the cycling process. In battery testing, the

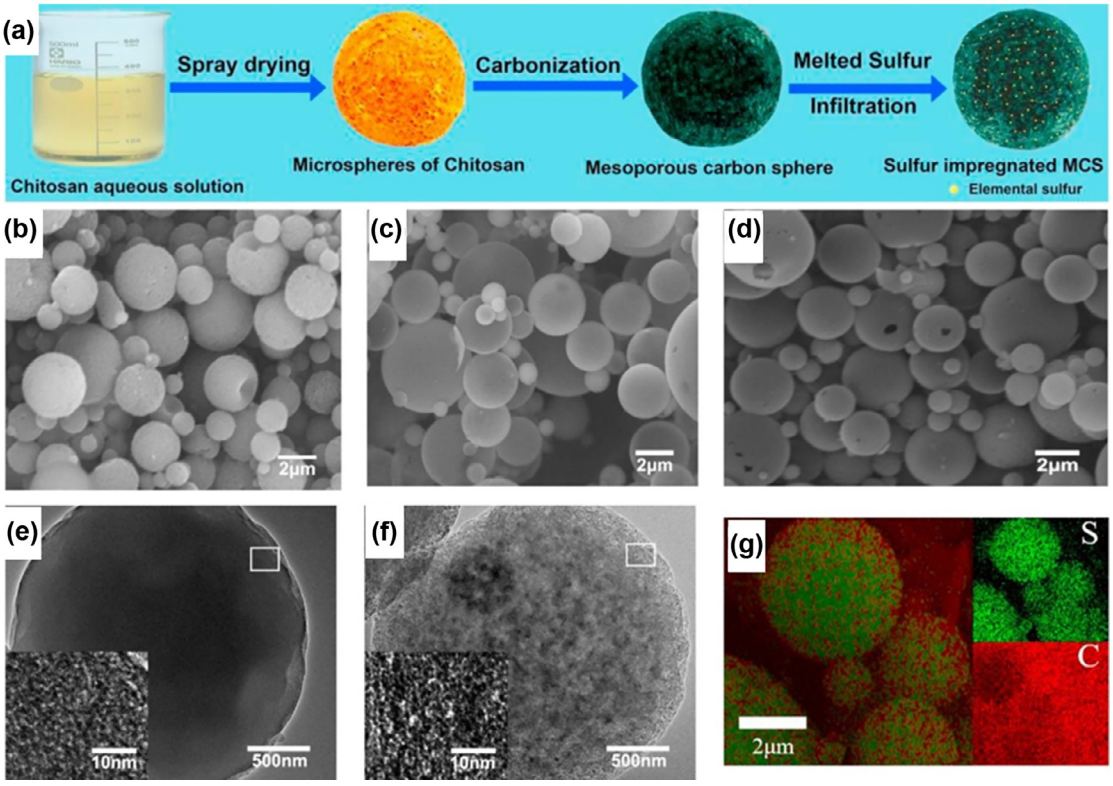

Fig. 6. (a) Illustration for the formation process of the S/MCS composite spheres; SEM images of MCS-0 (b), MCS-10 (c), MCS-20 (d) samples, TEM image of MCS-0 (e) and MCS-20 (f), and SEM image of S/MCS-20-50 (g) [97].

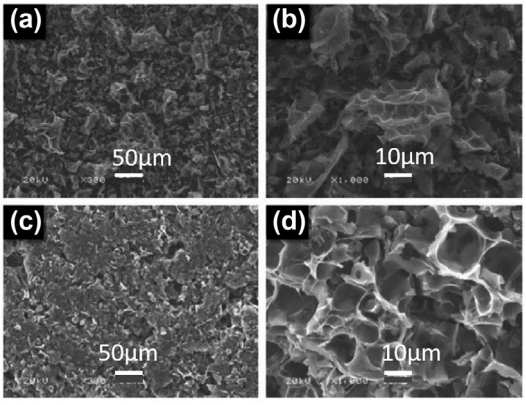

Fig. 7. SEM images of (a, b) the powder of cassava-carbon material (CCM) and (c, d) the surface of cassava-carbon sheets (CCS) [53].

composite materials revealed a high initial capacity of 1150 mAh/g as well as a reversible capacity of 613 mAh/g after the 100th cycle at 0.2 C.

Qin et al. [53] chose the thick roots of cassava as a carbon precursor and prepared a cassava-carbon sheet (CCS) as a polysulfides inhibitor between the cathode and the separator. The carbon was prepared by carbonizing the dry cassava under an argon atmosphere at 800 °C and was mixed with the polytetrafluoroethylene binder. Finally, the mixture was rolled into a membrane using a twin-roller and cut into circular sheets, which was placed between the sulfur cathode and the separator. It was found that the interconnected macroporous structure of CCS interlayers can provide a conductive framework to accommodate and reutilize polysulfides and confine them in the cathode side, just as shown in Fig. 7. In addition, the transfer of ions and electrons was enhanced because of the efficient accessibility of active material to the electrolyte and charge. The battery can hold a discharge capacity of 811 mAh/g after 100 cycles at 0.5 C and 640 mAh/g at 4 C, which exhibits excellent cycle stability and superior rate capability.

3.3. Biomass-derived carbon from high cellulose, hemi-cellulose and lignin plants

Cellulose, hemicellulose, and lignin are biomacromolecules synthesized by plants. Strictly speaking, they also belong to carbohydrates and have the high carbon content. For many plants, especially woody plants, their content reaches more than 90%, which is an ideal raw material for BDNCs. Using a large number of biomass wastes, such as peanut shells, orange peels, and leaves, the researchers have been able to produce carbon materials with hierarchical pore structure and obtain very high specific surface area, which can provide loading space for active materials in Li–S batteries and significantly improve the battery capacity. Their applications in Li–S batteries are shown in Table 3.

Fig. 8 shows that the carbon slices were synthesized by a facile carbonization using the bark of a plane tree as the renewable carbon source in our previous work [101]. The bark derived carbon has an integrated architecture carbon slices with interconnected porous structures including micropores, mesopores, and macropores. Moreover, the carbon–sulfur slice electrode could highly load sulfur of 3.2–4.2 mg/cm^2. Moreover, the integrated binder-free and conducting additive-free cathodes exhibited an excellent electrochemical performance for lithium sulfur batteries.

K. Balakumar et al. [77] employed a facile and bio-inspired safe technique to synthesize activated carbons with large pore volume (0.82 cm^3/g) and surface area (1952 m^2/g) from waste coir pith. The coir pith was firstly pyrolyzed at 350 °C and then mixed with KOH and heated at 800 °C to obtain activated porous carbon. The high surface area carbon acted as a potential host for sulfur with

Table 3. Porous carbons derived from high cellulose, hemi-cellulose and lignin biomass used as key materials and their properties for Li–S batteries.

Biomass source	Pore structure	Activating agent	Surface area (m^2/g)	Pore volume (cm^3/g)	Initial capacity (mAh/g)	Capacity retention (mAh/g)	Cycle number/ rate (C)	S (wt%)	Ref.
Coir pith	micropore	KOH	1952	0.86	1350	609	75/0.1	60	[77]
Peanut shell	micropore	K_2FeO_4	1373	0.65	1146	826	1000/1	50.5	[98]
Apricot shell	micropore	KOH	2269	1.05	1277	710	200/0.2	53.5	[99]
Mushroom	micropore	H_3PO_4	788	0.77	1357	852.2	50/0.3	52	[100]
Pomelo peel	micro-mesopore	KOH	1533	0.84	1258	750	100/0.2	60	[17]
Cyclosorus interruptus	hierarchical pore	$KHCO_3$	1549.7	0.88	1377	753	100/0.2	66.4	[82]
Walnut shell	hierarchical pore	KOH	2318	1.137	1350	910	100/0.1	48.8	[59]
Mandarin peel	hierarchical pore	K_2CO_3	1077	0.57	886	790	40/0.05	/	[77]
Banana peel	hierarchical pore	SiO_2	235	0.41	1100	707	100/0.2	67	[20]
Tree barks	hierarchical pore	/	528	0.72	1159	608	60/0.2	48	[101]
Rice husk	meso-macropore	KOH	1098.1	3.5	1230	/	//0.1	/	[21]
Rapeseed shell	macropore	KOH	2092	1.28	942	486	500/0.8	60	[102]
Leaf	micro-mesopore	/	390	0.34	1320	850	100/0.2	70	[103]
Enteromorpha	hierarchical pore	KOH	2086	0.89	1617	507.5	250/0.2	40	[104]
Luffa sponge*	micropore	KOH	3211.2	1.72	1544.2	976.6	200/0.2	70	[105]
Oak Tree fruit shells*	pore	KOH	796	0.37	1324	990	50/0.2	/	[22]
Corncob*	mirco-/mesopore	KOH	2645	1.54	1425.1	839.8	100/0.3	85.8	[106]
Bacterial cellulose*	3D structure layer by layer	TiO_2	/	/	1314	1048.5	50/0.2	/	[107]
Bamboo*	porous fibers	KOH	776.07	0.33	907	605	300/1	70	[19]

* Derived carbons used as interlayers.

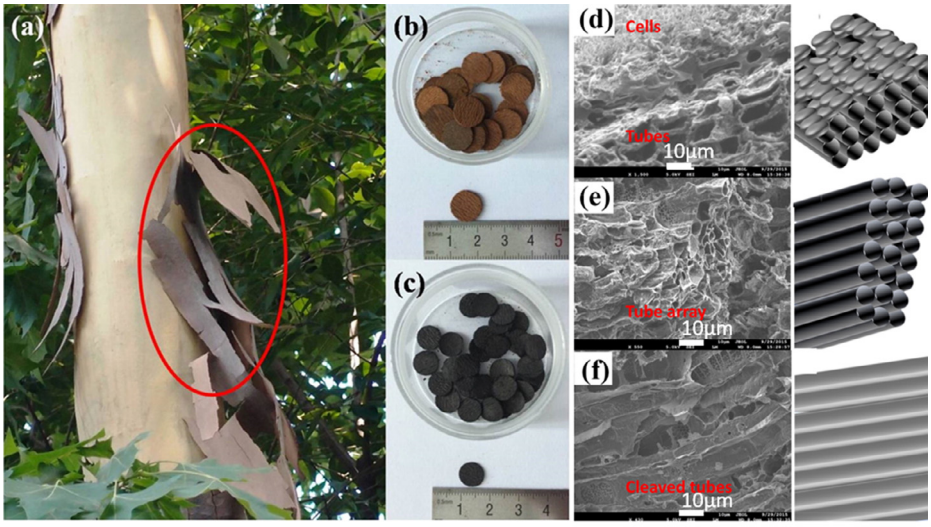

Fig. 8. Photographs of the fabrication process of integrated carbon slice electrodes: (a) bark of plane tree, (b) bark slices, and (c) carbonized bark slices; (d) FESEM image of outer layer and inter layer in carbonized plane tree bark and (e) its scheme. (f) Cross-section FESEM image of tube array and their schemes [101].

an ability to accommodate a maximum of 70 wt%, and it provided a desirable electronic/ionic transport path-way to sulfur and offered a favorable electrode-electrolyte interface for better electrochemical reaction. The microporous electrochemical reactors alleviated the polysulfide dissolution along with a cushioning effect to the electrode against volume change. As a result, the composite cathode tolerated 1 C rate condition and exhibited a progressive capacity of 695 mAh/g with 95% Coulombic efficiency after 50 cycles.

It is generally believed that due to the narrow space in microporous carbon, the movement of small sulfur molecules can be effectively restricted, thus avoiding the formation of soluble polysulfide. But this hypothesis still needs more experimental evidence to prove it. Zhou et al. [98] demonstrated the direct transformation of sulfur to smaller sulfur molecules by using ultramicroporous carbon as sulfur host and carbonate-based electrolyte as shown in Fig. 9. The microporous graphitic carbon was synthesized via the simultaneous activation and graphitization of peanut shell char promoted by K_2FeO_4, which possessed ultra-micropore (pore width < 0.7 nm) volume as high as 0.65 cm^3/g and the predominant pore width less than 0.4 nm. The mechanism of the composite formation was analyzed by using X-ray photoelectron spectroscopy (XPS) sputter profiling, which demonstrated that during the heat treatment, sulfur has been confined to the micropores of MGC to form a small chain-like S_{2-4} composite, and the ultramicropores with narrow width effectively inhibited the side reactions of S_{2-4} with carbonate solvents. The composite exhibited a superior long-term cycling and rate performance in the carbonate-based electrolyte. Discharge capacities of 826 and 571 mAh/g remained after 1000 cycles at 1 C and 2 C, respectively. In addition, a high capacity of 570 mAh/g is obtained at 4 C.

In order to transport necessary active substances, there are often some special channel structures inside the biomass. After the carbonization, the pore structure formed on these channels help to improve the battery capacity and cycle performance. You et al. [82] presented a facile one-step pyrolysis approach for synthesizing hierarchical porous carbon (HPC) with cyclosorus interruptus as a carbon source. Chemical activation was carried out by using $KHCO_3$. And the S/HPC was prepared by in situ redox reaction of $Na_2S_2O_3$ with acid in the presence of HPC. The obtained

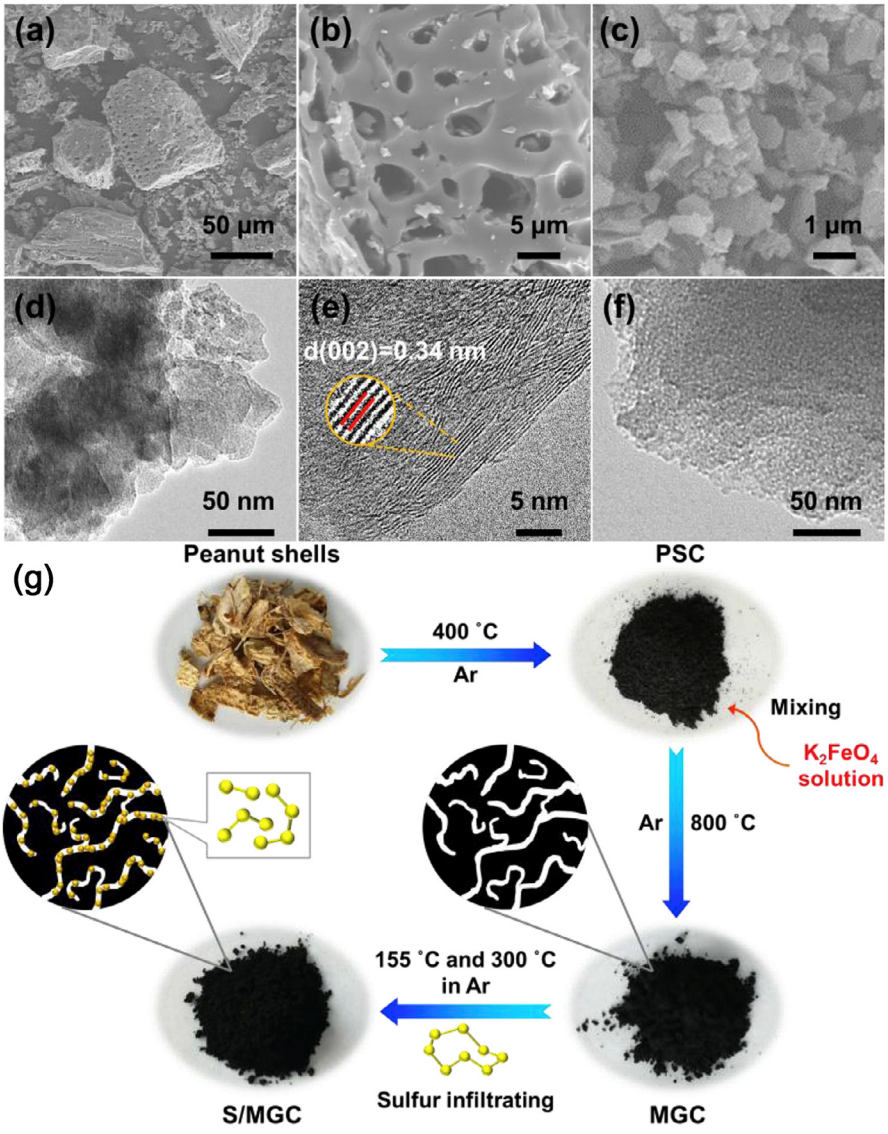

Fig. 9. SEM images of (a, b) MGC and (c) S/MGC; (d) TEM and (e) HR-TEM images of MGC; (f) TEM image of S/MGC; (g) the preparation process of the S/MGC composite [98].

HPC consisted of many regular macroporous channels and there were lots of hierarchical grating-like pores walls inside the channels, which were supposed to greatly facilitate the infiltration of the electrolyte and Li-ion. The HPC had a very large specific surface area of 1549.7 m^2/g and high total pore volume of 0.88 cm^3/g. At the same time, the HPC was mild co-doped by inherent S and O. The prepared S/ HPC cathode with 66.4% sulfur showed a high initial discharge capacity of 1377 mAh/g at 0.2 C and retained 753 mAh/g after 100 cycles.

Liu et al. [59] prepared activated carbon (AC) through a carbonization treatment and an activation procedure with KOH form a walnut shell. The AC showed hierarchical pores: 0.6 nm micropores, 2.7 nm mesopores and macropores with an average diameter of 50 nm, providing a large specific surface area of 2318 m^2/g. This highly porous AC was tested as a host material to encapsulate sulfur via a vapor phase infusion process, and the SEM image of AC-S composite exhibited a smooth and dense surface. In addition, some big holes in micrometer scale were remained after loading sulfur, while the macropores with a diameter of 50 nm were no longer observed on the surface. When the composite was introduced into the Li–S battery, the developed AC-S electrode showed a high initial specific capacity of 1350 mAh/g and good capacity retention over 100 cycles at 0.1 C.

Paulina Półrolniczak et al. [77] prepared a novel activated hierarchical carbon by means of chemical activation of waste mandarin peels with potassium carbonate. The synthesized material owns hierarchical micro-macroporous structure with the sponge-like arrangement of interconnected microfilaments. Composite sulfur cathode fabricated with the application of this carbon has been shown to exhibit a very large initial specific discharge capacity of 886 mAh/g at 0.1 C, which remained remarkably stable over subsequent 50 charge/discharge cycles (capacity loss by 1%). Excellent reversibility and cyclic stability of this composite cathode have been attributed to a unique combination of micro and macroporosity, as well as surface chemistry, allowing for the retention of the intermediate polysulfides within the carbon framework, without excessive dissolution in the bulk of electrolyte. The intimate contact of the sulfur provided by the large surface area and the functional groups on the activated carbon surface were favorable to good ion accessibility leading to enhanced cycle stability and micropores in the carbon can restrict the diffusion of the polysulfides during cycling.

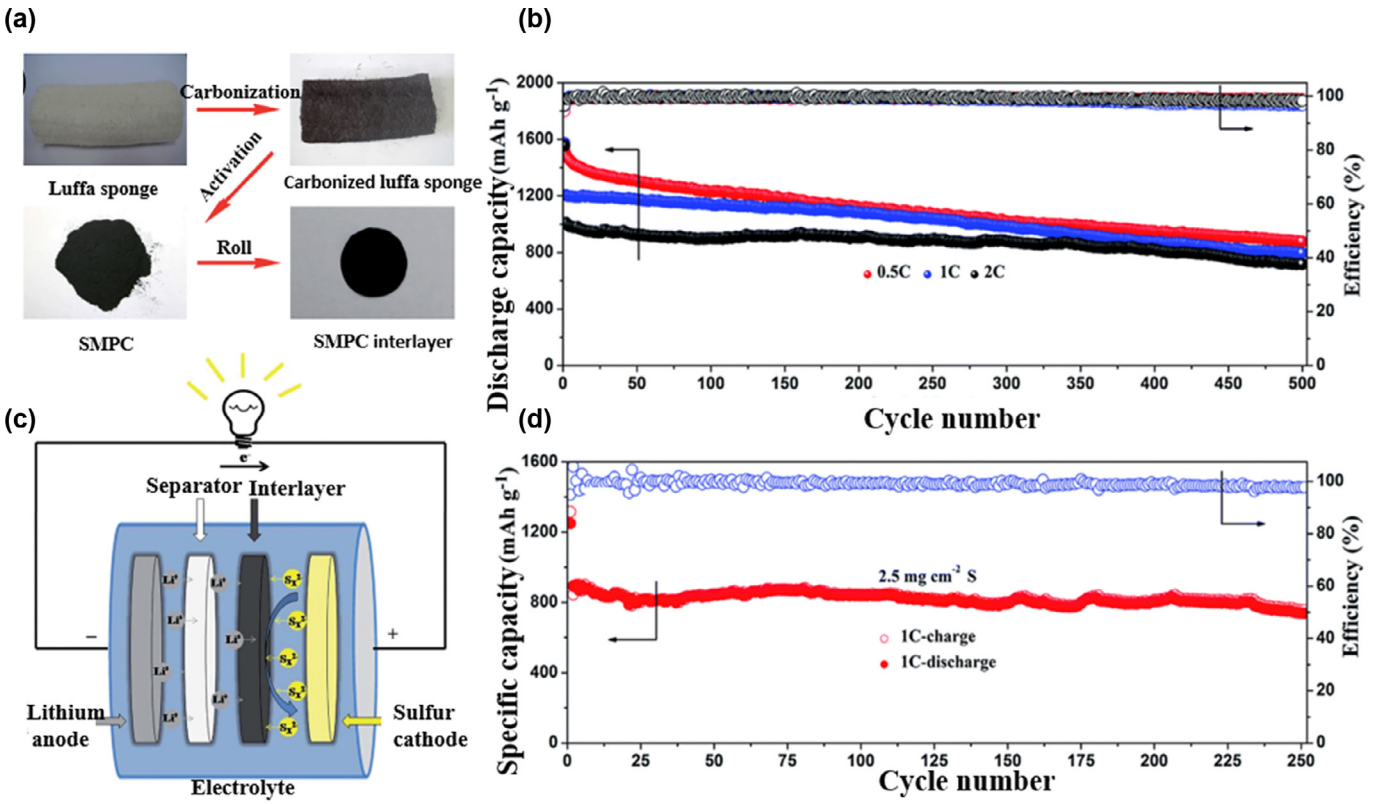

Fig. 10. (a) Schematic illustration for the formation of the SMPC interlayer. (b) Schematic cell configuration of the Li–S battery with SMPC interlayer. (c) The long cycling performance of the Li–S batteries with the SMPC interlayer at 0.5, 1 and 2 C. (d) Cycling performance of the Li–S batteries with the SMPC interlayer at 1 C [105].

Yang et al. [105] synthesized sulfur-doped microporous carbon (SMPC) from a renewable precursor, luffa sponge as shown in Fig. 10. The raw material is rich in C, S and O atoms, and thus can easily be converted into an in situ heteroatom-doped carbon material. The luffa sponge was carbonized directly with KOH as an activator at 800 °C. The obtained SMPC possessed a unique microporous carbon framework with a large specific surface area of 3211.2 m^2/g, high pore volume of 1.72 cm^3/g, good electrical conductivity of 1.89 S/cm, and in situ S-doping of 2.72 at%. The SMPC was mixed with PTFE binder and conductive carbon black at a mass ratio of 8:1:1, followed by roll-pressing and the interlayer was obtained. Due to the special physical properties and chemical ingredients of SMPC, the interlayer can offer more electrolyte infiltration and shorten the electron transfer path, which facilitates the mass transport of Li ions and conduction of electrons. At the same time, the combination of strong chemical and physical absorptions can immobilize active materials and restrict the dissolution of polysulfides. Thanks to these functional advantages, the battery exhibited a large reversible capacity of 1544.2 mAh/g at 0.2 C, a high rate capacity of 781.2 mAh/g at 5 C, and superior cyclability over 500 cycles at 2 C with 0.057% capacity fading per cycle.

Selvan et al. [22] explored biomass-derived porous carbon as polysulfide reservoir to modify the surface of glass fiber (GF) separator. They used Oak Tree fruit shells as a carbon source and discussed the different carbonization results from the process with and without KOH activation. They found electrochemical performance can be improved easily by a simple and straightforward coating of biomass-derived porous carbon onto the GF separator with an initial capacity of 1324 mAh/g at 0.2 C, which was 875 mAh/g for uncoated GF separator.

3.4. Biomass-derived carbon from high protein animal precursor

Protein is a biopolymer composed of amino acids. It is not only an important component of all cells, but also the main undertaker of life activities. It exists widely in animal skeletons, hair and other biological tissues. There are many kinds of proteins and their structures are complex. The content of carbon in protein is about 50%. After high-temperature decomposition, hierarchical porous derived carbon based on life tissue can be obtained. It can be used as the positive sulfur host and the raw material of special separator for Li–S batteries to improve its capacity and cycle performance. Their applications and other biomass used in Li–S batteries are shown in Table 4.

In order to further improve the electrochemical performance, many researchers suggested that N doping can be used to enhance the surface affinity of polysulfides [113]. Qu et al. [55] reported a novel highly ordered nitrogen-rich mesoporous carbon (HNMC) prepared by pyrolysis of gelatin and a simple template process. The carbon was activated with KOH and obtained the surface area of 2892.6 m^2/g with a pore volume of 2.80 cm^3/g. Through a simple melt-diffusion method, the obtained carbon showed acceptable up to 53.3 wt% S loading and a stable framework to limit the volume expansion and suppress the shuttle effect, which greatly improved the performance of batteries. It was found that the elemental sulfur can be homogeneously dispersed inside the mesopores of materials. Due to the increased surface adsorption via N-doping (9.74 at%), the diffusion of polysulfides was further inhibited. Electrochemical tests revealed that the composite owned high rate capability and long cycling stability as cathode materials, such as a high initial discharge capacity of 1209 mAh/g and retained

Table 4. Porous carbons derived from high protein animal precursor and other biomass used as key materials and their properties for Li–S batteries.

Biomass source	Obtained structure	Activating agent	Surface area (m^2/g)	Pore volume (cm^3/g)	Initial capacity (mAh/g)	Capacity retention (mAh/g)	Cycle number/ rate (C)	S (wt%)	Ref.
Gelatin	mesoporous	KOH	2892.6	2.8	1209	600	200/1	53.3	[55]
Goat hair	hierarchical porous carbon	H_3PO_4	535.4	0.39	1185	489	300/0.2	54.33	[84]
Silk cocoon	hierarchical porous carbon	$FeCl_3$ and $ZnCl_2$	1540	1.85	1303	594	100/0.5	5.7	[51]
Tuna bone	porous carbon	KOH	1517.	2.53	1397.5	599.9	700/1	84	[60]
Crab shells*	micro-/mesoporous	KOH	1298.2	2.1	1301	971.3	100/0.1	77	[108]
Novolac	microporous	CO_2	2080	1.45	884	604	100/0.1	54	[109]
Poplar catkin	hierarchically sponge-like	KOH	1261.7	0.62	1154	74	100/0.1	56.5	[110]
Green algae	hierarchical porous carbon	/	101	0.54	1327	757	100/0.1	63	[56]
Aspergillus flavus	porous carbon	KOH	2459.6	1.5	1625	940	120/0.2	56.7	[111]
Filamentous fungi*	meso-macropores	/	305	1.23	750	605	100/0.5	60	[112]

* Derived carbons used as interlayers.

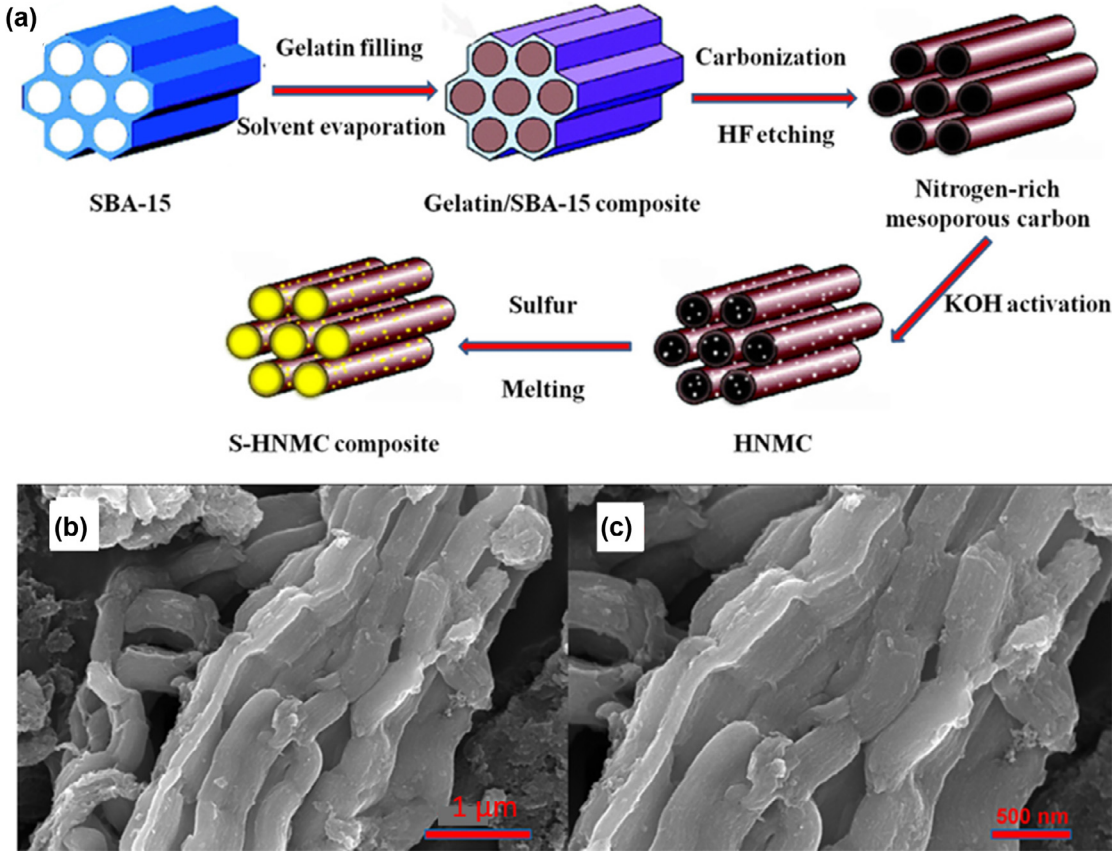

Fig. 11. (a) Schematic illustration of the synthesis procedure of the S–HNMC composite; (b, c) SEM images of the S–HNMC (53.3 wt% sulfur) composite [55].

as high as 600 mAh/g after 200 cycles at 1 C, as shown in Fig. 11. The results illustrated that encapsulating sulfur into the highly ordered nitrogen-rich mesoporous carbon nanostructure can contribute a lot to high rate capability and long-term cycling stability effectively.

Ren et al. [84] employed goat hair, as a low-cost and eco-friendly precursor to prepare cauliflower-like in-situ nitrogen, oxygen, and phosphorus tri-doped porous biomass carbon (NOPC) by carbonization process at 600 °C and a facile activation with H_3PO_4, as shown in Fig. 12. The obtained material possessed a 3D hierarchical porous structure with the high specific surface area (535.352 m^2/g), as well as good pore size distribution. The carbon and sulfur were compounded by a stem-melting technology as cathode materials of Li–S batteries. In the composite, electrons and ions transfer and utilization of active sulfur were improved due to the synergistic effect of special physical structure and inherent tri-doping of N, O, and P, and the shuttle behaviors of soluble lithium polysulfides were also mitigated. Moreover, the composite exhibited excellent electrochemical performance, with a high initial discharge capacity of 1185 mAh/g at 0.05 C and maintaining a relatively considerable capacity of 489 mAh/g at 0.2 C after 300 cycles.

Xiang et al. [51] prepared an in-situ nitrogen-doped porous carbon nanosheet (NPCN) materials derived from renewable silk cocoon via a facile simultaneous activation and carbonization approach using metal salt $FeCl_3$ and $ZnCl_2$ as chemical activating agents. As a comparison, silk cocoon derived carbon (SCC) without activation was also prepared. The obtained NPCN had a unique interconnected sheet-like morphology and a hierarchically porous structure with a relatively high specific surface area of 1540 m^2/g and a large pore volume of 1.85 cm^3/g. The resulting carbon/sulfur composite (NPCN/S) showed a remarkably improved rate performance and superior long-term cycling stability with an extremely low decay rate (0.1% per cycle) up to 300 cycles at a high rate of 2

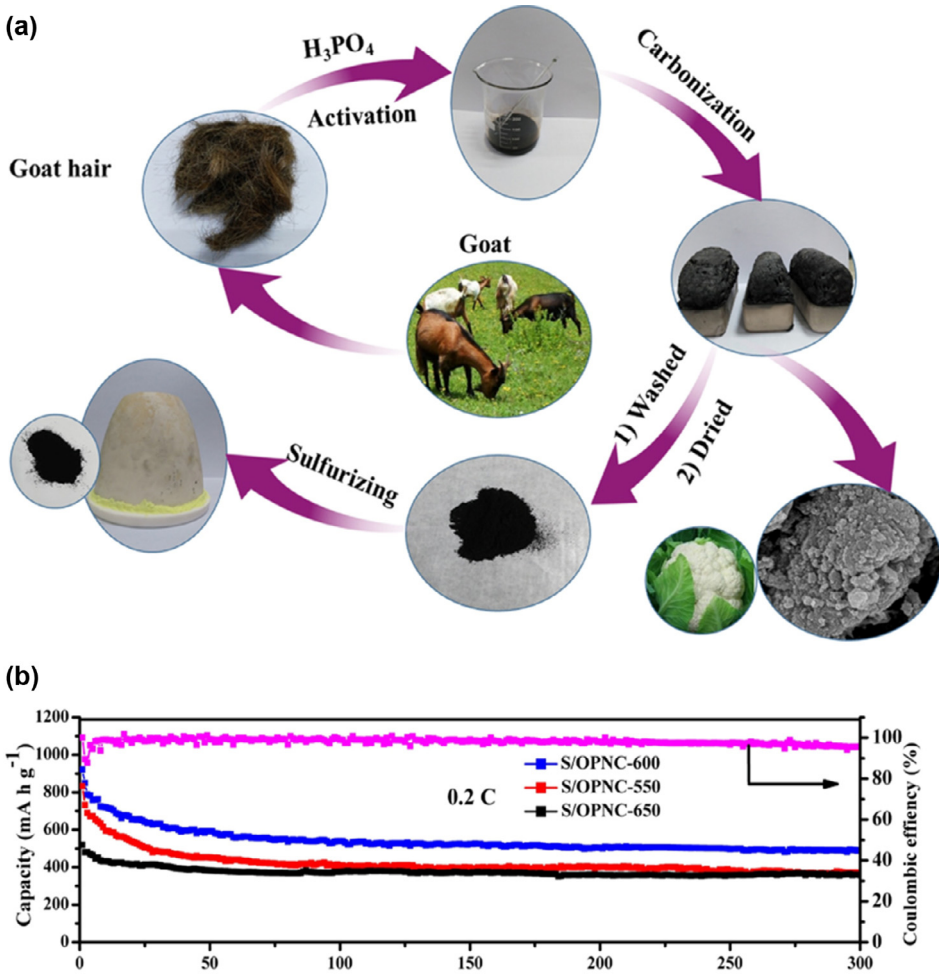

Fig. 12. (a) Schematic of the formation of S/NOPC composite materials; (b) Cycling performances of the S/NOPC-550, S/NOPC-600 and S/PPNC-650 composites at 0.2 C [84].

C as shown in Fig. 13. Active sulfur can be effectively encapsulated into the pores of the NPCN via a facile melt-diffusion strategy, and the sulfur loading in the NPCN/S composites can be easily adjusted from 55.7% up to 76.8%.

Shao et al. [61,108] chose crab shell as a precursor, obtained two different carbons: (1) novel nitrogen doped micro-/mesoporous carbon (N-MIMEC) and (2) $Ca(OH)_2$–carbon framework. Both carbons experienced high-temperature carbonization, while the N-MIMEC was obtained with KOH activation. The carbons were coated directly on one side of a separator (Celgard 2400) with different proportions of gelatin. They found the two carbons can facilitate electron and ion transfer during redox reactions and efficiently traps the dissolved polysulfides. In N-MIMEC, the micro-/mesopores provide enough surface area for sulfide adsorption and accommodate the volume change. The Li–S battery with an NMIMEC-coated separator exhibited excellent performance with an initial capacity of 1301 mAh/g and a high reversible capacity of 971.3 mAh/g after 100 cycles at 0.1 C. An enhanced Li–S performance is also achieved by the utilization of a $Ca(OH)_2$–carbon framework-modified separator, resulting in an initial capacity of 1215 mAh/g and a high reversible capacity of 873.5 mAh/g after 250 cycles at a rate of 0.5 C.

4. Economic benefits

In the first half of 2017, the global Li-ion battery revenue reached $17.8 billion [114]. However, the development of Li-ion batteries is limited by the disadvantages of poor safety, high cost and insufficient capacity. Therefore, as a new generation of lithium batteries, Li–S battery is becoming the focus of attention. As described before, the specific capacity of Li–S batteries is as high as 1675 mAh/g, which is much higher than that of lithium cobalt oxide batteries widely used commercially (<150 mAh/g). The theoretical energy density of rechargeable Li–S secondary batteries at room temperature is 2654 Wh/kg, which is 7 times that of Li-ion batteries ($LiCoO_2$/C, lithium removal 0.5, theoretical energy density 360 Wh/kg). Because of the absolute superiority of performance, if reliable Li–S batteries are commercially operated, they will quickly occupy or even replace the Li-ion battery market.

According to the market prices of cathode materials for lithium batteries, the prices of $LiNi_{1/3}Mn_{1/3}Co_{1/3}O_2$ (NMC333), NMC622, NMC811 and $LiMn_2O_4$ are $23,000, 22,100, 21,500 and 12,000 per ton respectively in the cathode material of commercial Li-ion batteries [115]. However, the price of sulfur in the cathode active material for Li-S batteries is stable at $450 per ton. Furthermore, China's sulfur output in 2017 has reached 5.8 million tons. If the effective utilization rate of active substance elemental sulfur can reach 60%, only 500 tons of elemental sulfur will be needed to produce 50 million Li–S secondary batteries for notebook computers [116]. In the other hand, the cost of advanced commercial carbon materials is high, such as carbon nanotube, macroporous carbon and graphene. As the main component of cathode materials, we introduce BDNCs into Li–S battery system, which further improve the performance of batteries, and the cost is further short-

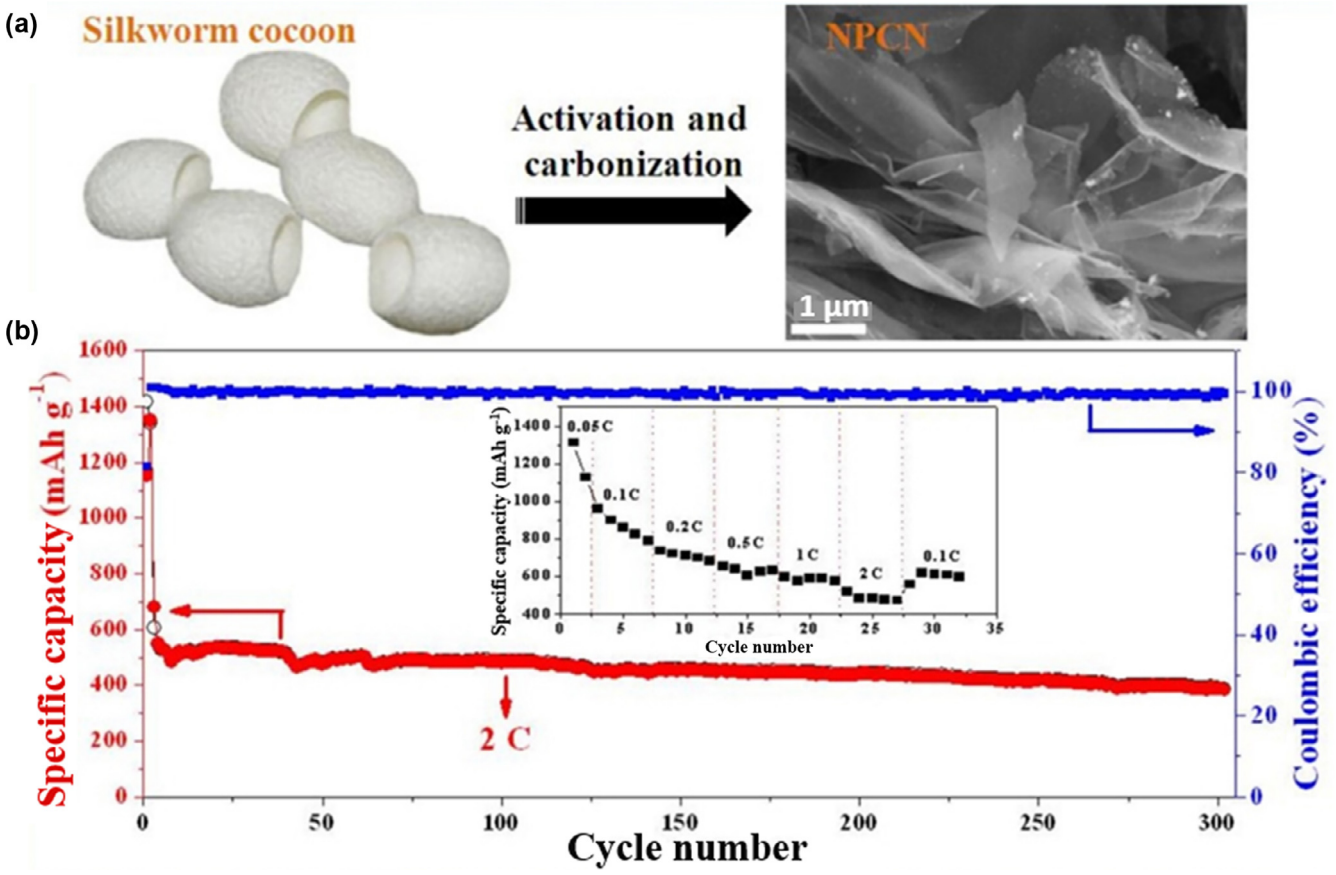

Fig. 13. (a) Schematic illustration of preparation processes of NPCN composites and (b) long-term cycling performance of the NPCN/S-55.7 electrode at a high rate of 2 C after two cycles at 0.05 C [51].

ened. Compared with new carbon materials such as graphene and carbon nanotubes, most of the raw materials used in BDNCs are agricultural wastes, so the cost of them is almost negligible.

Besides material cost, the cost of carbonization process is also an important economic factor. At present, there are already very mature biomass pyrolysis technology applications in the biomass power generation industry, through the transformation of existing equipment and technology can easily achieve fast and inexpensive biomass-derived carbons [117]. However, as mentioned above, the direct carbonization method cannot get ideal BDNCs for Li-S batteries. It is necessary to pre-carbonize the raw materials at high temperature and then add appropriate activation process. Usually physical activation method has low cost. Some cheap chemical activators such as NaOH and K_2CO_3 are more suitable for industrial carbon activation process. The hydrothermal carbonization process always needs special high-pressure reactor because of the requirement of reaction environment, and it is not suitable for large-scale industrial production [118]. Other carbonization methods such as microwave carbonization and plasma carbonization are more expensive because of their immature technology.

With the increasing demand for high-density energy storage in the market, Li–S batteries based on BDNCs have huge market prospects, which can bring enormous economic benefits while making full use of biological waste and protecting the environment.

5. Conclusions and outlook

Biomass, as the most widely used source of carbon, has great potential applications in energy storage devices. Thanks to their rich resources, environmental friendliness, and adjustable physical/chemical properties, the BDNCs are considered the next excellent candidates of key materials for Li–S batteries. In this view, we presented recent progress in BDNCs from different biomasses used as cathode materials and interlayers in high-performance Li–S batteries. Carbons with different structures (microporous, mesoporous, hierarchical porous) and preparation methods have been introduced in this article. In addition, we discussed the effects of pore structure, surface area and heteroatom doping of the carbons on the electrochemical properties of Li–S batteries as well as general synthetic methods for BDNCs. Finally, we also compared Li–S batteries with commercially available Li-ion batteries and analyzed the market prospects of BDNCs for Li–S batteries.

From the point of view of biomass, waste biomass rich in cellulose, hemicellulose and lignin are the best raw materials for BDNCs, because they are usually cheaper, and the properties of the materials are relatively stable. They usually have high relative specific surface area and porous nanostructures, which can effectively improve the capacity and cycle performance of batteries. Although plants with high sugar and starch can produce BDNCs with smaller pore size, which can effectively limit shuttle effect, they will not be the preferred commercial Li–S batteries in the future because their specific surface area is usually not high enough and the cost is relatively high. BDNCs made from high-protein animal waste usually have similar structures to high-cellulose derived carbon, and they also have the potential to become commercial electrode materials for Li–S batteries.

Although obvious progress in Li–S batteries has been made by employing novel BDNCs from their excellent electrochemical performance, there are some challenges such as long cycling performance, energy density, safety, and low S loading still need to improve for actual applications [119]. Considering that the production

process of BDNCs usually requires high-temperature carbonization, we must try to reduce energy consumption in this process. Moreover, some additives such as binders and conductive carbon black can influence battery capacity [120–122].

In order to solve the problems mentioned above, the new generation of BDNCs for Li–S batteries should concentrate on: (1) Rational regulation and control of structure and surface chemistry of BDNCs. The hierarchically porous carbon-containing micropores outside and meso/macropores inside could be a very good choice, in which the micropores serve as polysulfides inhibitor and the meso/macropores help high sulfur loading as well as fluent ion and electrolyte transport. Moreover, the chemical interactions between sulfur need to be enhanced to promote polar-polar interaction with lithium polysulfides, and heteroatom-doping would be an effective way to modify the surface chemistry of carbons. (2) Explore more environmentally friendly and energy-saving carbonation methods. The carbonization temperature of many reports is as high as 800 °C, which consume a lot of electrical energy and experimental time. Some activators such as KOH and $ZnCl_2$ also increase the cost of materials. Therefore, cheaper and more efficient activators should be found and the carbonization method at lower temperatures should be studied. (3) Expand the scale of biomass-derived carbon production from the laboratory stage to the actual industrial application.

We think that the electrochemical performance of Li–S batteries can be greatly improved with low cost as BDNCs could be effectively improved as described above. We hope that this review could provide an assistance for researchers to obtain cheaper and better biomass-derived carbons and further promote the commercialization of Li–S batteries.

Acknowledgments

This research was supported by the National Natural Science Foundation of China (U1832136 and 21303038), Think-Tank Union Funds for Energy Storage (Grant No.JZ2016QTXM1097), Open Funds of the State Key Laboratory of Rare Earth Resource Utilization (Grant No. RERU2016004), the Fundamental Research Funds for the Central Universities (JZ2016HGTA0690), Natural Science Foundation of Anhui province (1808085QE140), and 100 Talents Plan of Anhui.

References

[1] L. Jiang, L. Sheng, Z. Fan, Sci. China Mater. 61 (2017) 133–158.
[2] M. Legarra, T. Morgan, S. Turn, L. Wang, Ø. Skreiberg, M.J. Antal, Energy Fuels 32 (2017) 475–489.
[3] F. Yin, X. Liu, Y. Zhang, Y. Zhao, A. Menbayeva, Z. Bakenov, X. Wang, Solid State Sci. 66 (2017) 44–49.
[4] X. Li, N. Fu, J. Zou, X. Zeng, Y. Chen, L. Zhou, H. Huang, Mater. Lett. 209 (2017) 505–508.
[5] R. Fang, S. Zhao, S. Pei, X. Qian, P.X. Hou, H.M. Cheng, C. Liu, F. Li, ACS nano 10 (2016) 8676–8682.
[6] L. Sun, M. Li, Y. Jiang, W. Kong, K. Jiang, J. Wang, S. Fan, Nano Lett. 14 (2014) 4044–4049.
[7] T.N. Hoheisel, S. Schrettl, R. Szilluweit, H. Frauenrath, Angew. Chem. Int. Ed. 49 (2010) 6496–6515.
[8] W. Yang, K.R. Ratinac, S.P. Ringer, P. Thordarson, J.J. Gooding, F. Braet, Angew. Chem. Int. Ed. 49 (2010) 2114–2138.
[9] W. Tang, Y. Zhang, Y. Zhong, T. Shen, X. Wang, X. Xia, J. Tu, Mater. Res. Bull. 88 (2017) 234–241.
[10] C. Rodriguez Correa, T. Otto, A. Kruse, Biomass Bioenergy 97 (2017) 53–64.
[11] Y.-P. Gao, Z.-B. Zhai, K.-J. Huang, Y.-Y. Zhang, New J. Chem. 41 (2017) 11456–11470.
[12] O. Ioannidou, A. Zabaniotou, Renew. Sustain. Energy Rev. 11 (2007) 1966–2005.
[13] S. Imtiaz, J. Zhang, Z.A. Zafar, S. Ji, T. Huang, J.A. Anderson, Z. Zhang, Y. Huang, Sci. China Mater. 59 (2016) 389–407.
[14] G. Ren, S. Li, Z.-X. Fan, J. Warzywoda, Z. Fan, J. Mater. Chem. A 4 (2016) 16507–16515.
[15] J. Xu, H. Fan, D. Su, G. Wang, J. Alloy. Comp. 747 (2018) 283–292.
[16] Y. Liu, G. Li, J. Fu, Z. Chen, X. Peng, Angew. Chem. Int. Ed. 56 (2017) 6176–6180.
[17] J. Zhang, J. Xiang, Z. Dong, Y. Liu, Y. Wu, C. Xu, G. Du, Electrochim. Acta 116 (2014) 146–151.
[18] J. Guo, J. Zhang, F. Jiang, S. Zhao, Q. Su, G. Du, Electrochim. Acta 176 (2015) 853–860.
[19] X. Gu, C. Lai, F. Liu, W. Yang, Y. Hou, S. Zhang, J. Mater. Chem. A 3 (2015) 9502–9509.
[20] F. Li, F. Qin, K. Zhang, J. Fang, Y. Lai, J. Li, J. Power Sources 362 (2017) 160–167.
[21] K. Chen, D. Xue, Chinese J. Chem. 35 (2017) 861–866.
[22] R.K. Selvan, P. Zhu, C. Yan, J. Zhu, M. Dirican, A. Shanmugavani, Y.S. Lee, X. Zhang, J. Colloid Interface Sci. 513 (2018) 231–239.
[23] Y.X. Yin, S. Xin, Y.G. Guo, L.J. Wan, Angew. Chem. Int. Ed. 52 (2013) 13186–13200.
[24] R.F. Service, Science (2018) 1080–1081.
[25] A. Manthiram, S.H. Chung, C. Zu, Adv. Mater. 27 (2015) 1980–2006.
[26] H.-J. Peng, J.-Q. Huang, X.-B. Cheng, Q. Zhang, Adv. Energy Mater. 7 (2017) 1700260.
[27] G. Xu, B. Ding, J. Pan, P. Nie, L. Shen, X. Zhang, J. Mater. Chem. A 2 (2014) 12662–12676.
[28] R.P. Fang, S.Y. Zhao, Z.H. Sun, W. Wang, H.M. Cheng, F. Li, Adv. Mater. 29 (2017) 1606823.
[29] T.Z. Hou, W.T. Xu, X. Chen, H.J. Peng, J.Q. Huang, Q. Zhang, Angew. Chem. Int. Ed. 56 (2017) 8178–8182.
[30] M. Liu, X.Y. Qin, Y.B. He, B.H. Li, F.Y. Kang, J. Mater. Chem. A 5 (2017) 5222–5234.
[31] D. Bresser, S. Passerini, B. Scrosati, Chem. Commun. 49 (2013) 10545–10562.
[32] A. Manthiram, Y. Fu, S.H. Chung, C. Zu, Y.S. Su, Chem. Rev. 114 (2014) 11751–11787.
[33] K. Zhou, X. Fan, X. Wei, J. Liu, Sci. China Technol. Sci. 60 (2017) 175–185.
[34] X. Fan, W. Sun, F. Meng, A. Xing, J. Liu, Green Energy Environ. 3 (2018) 2–19.
[35] Z. Li, Y. Huang, L. Yuan, Z. Hao, Y. Huang, Carbon 92 (2015) 41–63.
[36] L. Borchardt, M. Oschatz, S. Kaskel, Chem-Eur. J. 22 (2016) 7324–7351.
[37] Z.W. Seh, Y. Sun, Q. Zhang, Y. Cui, Chem. Soc. Rev. 45 (2016) 5605–5634.
[38] M.F. Chen, S.X. Jiang, S.Y. Cai, X.Y. Wang, K.X. Xiang, Z.Y. Ma, P. Song, A.C. Fisher, Chem. Eng. J. 313 (2017) 404–414.
[39] X. Chen, H.J. Peng, R. Zhang, T.Z. Hou, J.Q. Huang, B. Li, Q. Zhang, ACS Energy Lett. 2 (2017) 795–801.
[40] G.Q. Tan, R. Xu, Z.Y. Xing, Y.F. Yuan, J. Lu, J.G. Wen, C. Liu, L. Ma, C. Zhan, Q. Liu, T.P. Wu, Z.L. Jian, R. Shahbazian-Yassar, Y. Ren, D.J. Miller, L.A. Curtiss, X.L. Ji, K. Amine, Nat. Energy 2 (2017) 17090.
[41] J. Liang, Z.-H. Sun, F. Li, H.-M. Cheng, Energy Storage Mater. 2 (2016) 76–106.
[42] P. Kalyani, A. Anitha, Int. J. Hydrogen Energy 38 (2013) 4034–4045.
[43] P. McKendry, Bioresource Technol. (2002) 37–46.
[44] C.-M. Liu, S.-Y. Wu, Renew. Energy 96 (2016) 1056–1062.
[45] F. Zheng, D. Liu, G. Xia, Y. Yang, T. Liu, M. Wu, Q. Chen, J. Alloys and Comp. 693 (2017) 1197–1204.
[46] Y. Li, S.X. Chang, L. Tian, Q. Zhang, Soil Biol. Biochem. 121 (2018) 50–58.
[47] X. Zhou, H. Zhu, Y. Wen, U.M. Goodale, X. Li, Y. You, D. Ye, H. Liang, Forest Ecol. Manag. 410 (2018) 164–173.
[48] X. Yang, Y. Jiang, R. Su, G. Yang, B. Xue, F. Li, Colloid. Surface. A 509 (2016) 314–322.
[49] D. Qin, S. Chen, J. Solid State Electrochem. 21 (2016) 1305–1312.
[50] M. Yu, R. Li, Y. Tong, Y. Li, C. Li, J.-D. Hong, G. Shi, J. Mater. Chem. A 3 (2015) 9609–9615.
[51] M. Xiang, Y. Wang, J. Wu, Y. Guo, H. Wu, Y. Zhang, H. Liu, Electrochim. Acta 227 (2017) 7–16.
[52] S. Li, J. Warzywoda, S. Wang, G. Ren, Z. Fan, Carbon 124 (2017) 212–218.
[53] F. Qin, K. Zhang, J. Fang, Y. Lai, Q. Li, Z. Zhang, J. Li, New J. Chem. 38 (2014) 4549–4554.
[54] Z. Sun, S. Wang, L. Yan, M. Xiao, D. Han, Y. Meng, J. Power Sources 324 (2016) 547–555.
[55] Y. Qu, Z. Zhang, X. Zhang, G. Ren, Y. Lai, Y. Liu, J. Li, Carbon 84 (2015) 399–408.
[56] Y. Zhao, X. Zhang, Y. He, N. Liu, T. Tan, C. Liang, Materials 10 (2017) 1158.
[57] M. Xue, C. Chen, Z. Ren, Y. Tan, B. Li, C. Zhang, Mater. Lett. 209 (2017) 594–597.
[58] M. Xue, C. Chen, Y. Tan, Z. Ren, B. Li, C. Zhang, J. Mater. Sci. 53 (2018) 11062–11077.
[59] Y. Jin, G. Zhou, F. Shi, D. Zhuo, J. Zhao, K. Liu, Y. Liu, C. Zu, W. Chen, R. Zhang, X. Huang, Y. Cui, Nat. Commun. 8 (2017) 462.
[60] F. Ai, N. Liu, W. Wang, A. Wang, F. Wang, H. Zhang, Y. Huang, Electrochim. Acta 258 (2017) 80–89.
[61] H. Shao, F. Ai, W. Wang, H. Zhang, A. Wang, W. Feng, Y. Huang, J. Mater. Chem. A 5 (2017) 19892–19900.
[62] T. Yin, Y. Wang, L. He, X. Gong, Comp. Mater. Sci. 138 (2017) 27–33.
[63] H. Luo, Y. Yang, X. Zhao, J. Zhang, Y. Chen, Electrochim. Acta 169 (2015) 13–21.
[64] A.H. Tchapda, V. Krishnamoorthy, Y.D. Yeboah, S.V. Pisupati, J. Anal. Appl. Pyrol. 128 (2017) 379–396.
[65] J.C. Yu-Chuan Lin, GeoffreyA. Tompsett, PhillipR. Westmoreland, GeorgeW. Huber, J. Phys. Chem. C (2009) 20097–20107.
[66] S. Inoue, Carbon 104 (2016) 263.
[67] B. Hu, K. Wang, L. Wu, S.H. Yu, M. Antonietti, M.M. Titirici, Adv. Mater. 22 (2010) 813–828.
[68] M. Sevilla, J.A. Maciá-Agulló, A.B. Fuertes, Biomass Bioenergy 35 (2011) 3152–3159.
[69] K. Tekin, S. Karagöz, S. Bektaş, Renew. Sustain. Energy Rev. 40 (2014) 673–687.
[70] A. Jain, R. Balasubramanian, M.P. Srinivasan, Chem. Eng. J. 283 (2016) 789–805.

[71] A. Jain, S. Jayaraman, R. Balasubramanian, M.P. Srinivasan, J. Mater. Chem. A 2 (2014) 520–528.
[72] C. Falco, J.P. Marco-Lozar, D. Salinas-Torres, E. Morallón, D. Cazorla-Amorós, M.M. Titirici, D. Lozano-Castelló, Carbon 62 (2013) 346–355.
[73] C. Falco, N. Baccile, M.-M. Titirici, Green Chem. 13 (2011) 3273.
[74] T. Tay, S. Ucar, S. Karagoz, J. Hazard. Mater. 165 (2009) 481–485.
[75] P. Williams, A. Reed, Biomass Bioenergy 30 (2006) 144–152.
[76] O. Sahin, C. Saka, Bioresoures Technol. 136 (2013) 163–168.
[77] P. Półrolniczak, P. Nowicki, K. Wasiński, R. Pietrzak, M. Walkowiak, Solid State Ionics 297 (2016) 59–63.
[78] X. Yuan, B. Liu, J. Xu, X. Yang, K. Zeinu, X. He, L. Wu, J. Hu, J. Yang, J. Xie, RSC Adv. 7 (2017) 13595–13603.
[79] J. Wang, S. Kaskel, J. Mater. Chem. 22 (2012) 23710.
[80] B. Xu, Y. Chen, G. Wei, G. Cao, H. Zhang, Y. Yang, Mater. Chem. Phys. 124 (2010) 504–509.
[81] D. Xu, C. Chen, J. Xie, B. Zhang, L. Miao, J. Cai, Y. Huang, L. Zhang, Adv. Energy Mater. 6 (2016) 1501929.
[82] X.-l. You, L.-j. Liu, M.-y. Zhang, M.D. Walle, Y. Li, Y.-N. Liu, Mater. Lett. 217 (2018) 167–170.
[83] Y. Zhao, L. Wang, L. Huang, M.Y. Maximov, M. Jin, Y. Zhang, X. Wang, G. Zhou, Nanomaterials 7 (2017) 402.
[84] J. Ren, Y. Zhou, H. Wu, F. Xie, C. Xu, D. Lin, J. Energy Chem. (2018), doi:10.1016/j.jechem.2018.01.015.
[85] A.A. Salema, F.N. Ani, Bioresource Technol. 102 (2011) 3388–3395.
[86] J. Zhu, S. Pallavkar, M. Chen, N. Yerra, Z. Luo, H.A. Colorado, H. Lin, N. Haldolaarachchige, A. Khasanov, T.C. Ho, D.P. Young, S. Wei, Z. Guo, Chem. Commun. 49 (2013) 258–260.
[87] C.T. Fleaca, F. Dumitrache, I. Morjan, R. Alexandrescu, I. Sandu, C. Luculescu, S. Birjega, G. Prodan, I. Stamatin, Appl. Surf. Sci. 258 (2012) 9394–9398.
[88] C.-F.W. Jing Wang, Su Chen, Angew. Chem. Int. Ed. (2012) 9297–9301.
[89] C. Barchasz, F. Molton, C. Duboc, J.C. Lepretre, S. Patoux, F. Alloin, Anal. Chem. 84 (2012) 3973–3980.
[90] D. Zheng, X. Zhang, J. Wang, D. Qu, X. Yang, D. Qu, J. Power Sources 301 (2016) 312–316.
[91] Y. Yang, G. Zheng, Y. Cui, Chem. Soc. Rev. 42 (2013) 3018–3032.
[92] E.P. Kamphaus, P.B. Balbuena, J. Phys. Chem. C 120 (2016) 4296–4305.
[93] Y.V. Mikhaylik, J.R. Akridge, J. Electrochem. Soc. 151 (2004) A1969.
[94] K. Kumaresan, Y. Mikhaylik, R.E. White, J. Electrochem. Soc. 155 (2008) A576.
[95] Z.W. Seh, Q. Zhang, W. Li, G. Zheng, H. Yao, Y. Cui, Chem. Sci. 4 (2013) 3673.
[96] G. Zheng, Q. Zhang, J.J. Cha, Y. Yang, W. Li, Z.W. Seh, Y. Cui, Nano. Lett. 13 (2013) 1265–1270.
[97] H. Zhou, D. Wang, A. Fu, X. Liu, Y. Wang, Y. Li, P. Guo, H. Li, X.S. Zhao, Mater. Sci. Eng. B 227 (2018) 9–15.
[98] J. Zhou, Y. Guo, C. Liang, J. Yang, J. Wang, Y. Nuli, Electrochim. Acta 273 (2018) 127–135.
[99] K. Yang, Q. Gao, Y. Tan, W. Tian, L. Zhu, C. Yang, Micropor. Mesopor. Mat. 204 (2015) 235–241.
[100] H. Wu, Y. Deng, J. Mou, Q. Zheng, F. Xie, E. Long, C. Xu, D. Lin, Electrochim. Acta 242 (2017) 146–158.
[101] J. Xu, K. Zhou, F. Chen, W. Chen, X. Wei, X.-W. Liu, J. Liu, ACS Sustain. Chem. Eng. 4 (2016) 666–670.
[102] M. Zheng, Q. Hu, S. Zhang, H. Tang, L. Li, H. Pang, Appl. Sci. 7 (2017) 1036.
[103] S.H. Chung, A. Manthiram, ChemSusChem 7 (2014) 1655–1661.
[104] S. Ji, S. Imtiaz, D. Sun, Y. Xin, Q. Li, T. Huang, Z. Zhang, Y. Huang, Chem-Eur. J. 23 (2017) 18208–18215.
[105] J. Yang, F. Chen, C. Li, T. Bai, B. Long, X. Zhou, J. Mater. Chem. A 4 (2016) 14324–14333.
[106] Z. Xu, Int. J. Electrochem. Sci. (2017) 4515–4527.
[107] F. Li, G. Wang, P. Wang, J. Yang, K. Zhang, Y. Liu, Y. Lai, J. Electroanal. Chem. 788 (2017) 150–155.
[108] H. Shao, B. Huang, N. Liu, W. Wang, H. Zhang, A. Wang, F. Wang, Y. Huang, J. Mater. Chem. A 4 (2016) 16627–16634.
[109] S. Choudhury, B. Krüner, P. Massuti-Ballester, A. Tolosa, C. Prehal, I. Grobelsek, O. Paris, L. Borchardt, V. Presser, J. Power Sources 357 (2017) 198–208.
[110] Y. Zhao, J. Ren, T. Tan, M.R. Babaa, Z. Bakenov, N. Liu, Y. Zhang, Nanomaterials 7 (2017) 260.
[111] M. Xu, M. Jia, C. Mao, S. Liu, S. Bao, J. Jiang, Y. Liu, Z. Lu, Sci. Rep. 6 (2016) 18739.
[112] L. Zhang, Y. Wang, B. Peng, W. Yu, H. Wang, T. Wang, B. Deng, L. Chai, K. Zhang, J. Wang, Green. Chem. 16 (2014) 3926.
[113] Z. Geng, Q. Xiao, D. Wang, G. Yi, Z. Xu, B. Li, C. Zhang, Electrochim. Acta 202 (2016) 131–139.
[114] G. Martin, L. Rentsch, M. Höck, M. Bertau, Energy Storage Mater. 6 (2017) 171–179.
[115] S. Ahmed, P.A. Nelson, K.G. Gallagher, N. Susarla, D.W. Dees, J. Power Sources 342 (2017) 733–740.
[116] X.Q. Xiu, J.L. Li, D. Hui, Appl. Mech. Mater. 291-294 (2013) 627–631.
[117] T. Gebreegziabher, A.O. Oyedun, H.T. Luk, T.Y.G. Lam, Y. Zhang, C.W. Hui, Chem. Eng. Res. Des 92 (2014) 1412–1427.
[118] M. Lucian, L. Fiori, Energies 10 (2017) 211.
[119] Q.Z. Hong-Jie Peng, Angew. Chem. Int. Ed. (2015) 11018–11020.
[120] Q. Pang, X. Liang, C.Y. Kwok, L.F. Nazar, J. Electrochem. Soc. 162 (2015) A2567–A2576.
[121] X. Liang, A. Garsuch, L.F. Nazar, Angew. Chem. Int. Ed. 54 (2015) 3907–3911.
[122] J. Deng, M. Li, Y. Wang, Green Chem. 18 (2016) 4824–4854.